

# The Scimitar Precooled Mach 5 Engine

*F. Jivraj\*, R. Varvill\*, A. Bond\* and G. Paniagua\*\**

*\*Reaction Engines Ltd*

*Culham Science Centre, Abingdon, Oxon, OX14 3DB, UK*

*\*\*von Karman Institute for Fluid Dynamics*

*Chaussée de Waterloo 72, B – 1640 Rhode-Saint-Genèse, Belgique*

## Abstract

Scimitar is a hypersonic air-breathing engine, which allows for active compression through the use of advanced heat exchangers. The Mach number limitation associated with gas turbines can therefore be overcome by “precooling” the inlet air prior to compression. Hydrogen fuel is used as a heat rejection sink in a complex thermodynamic cycle to allow the incoming air to be cooled adequately; the actual cycle working fluid is high-pressure helium, a good heat and work transfer medium. In what follows, the theory behind the thermodynamic cycle is presented, together with the practical technology being developed to prove and explore Scimitar’s feasibility.

## 1. Introduction

The Scimitar precooled Mach 5 cruise engine has been derived from the Reaction Engines SABRE engine designed to propel the SKYLON SSTO spaceplane. These engines are able to achieve high-speed air-breathing flight by using hydrogen fuel as a heat sink to lower the temperature of the decelerated inlet air so that it can be compressed and managed through combustion by relatively conventional turbo-machinery. The fluid flow is entirely subsonic while passing through the cycle, being supersonic only in the intake capture and nozzle acceleration phases.

Through clever thermodynamic design, it is also able to cruise effectively at Mach 0.9, with a range close to that when in supersonic mode. This not only allows the vehicle to come out of supersonic flight and continue at subsonic speeds during for example equipment failures; but more importantly it allows the vehicle to fly overland subsonically, eliminating the noise issues due to sonic booms. A subsonic exhaust at take-off has also been incorporated even though it is operating with reheat at the time, it therefore fully meets all current civil aviation legislation, hence overcoming a major operational obstacle which hindered Concorde.

As for the fuel, liquid hydrogen is used for two main reasons. Firstly, it has a large calorific value (120MJ/kg) which allows for an antipodal range if the engine can be realised with near ideal theoretical performance for cruise at Mach 5. For an airframe with an L/D of about 6, this would give a nominal flight time of 4 hours, or less, to anywhere in the world. Secondly, although liquid hydrogen is a hard cryogen (having a low density of 68kg/m<sup>3</sup> at a boiling point of only 21K), it has a very high thermal capacity, almost 3.5 times that of water. If stored at low enough temperatures to maintain its state, it can therefore be used to effect the precooling of the air entering the compressor up to Mach 5, while maintaining an equivalence ratio close to that for optimum performance. Hence, the liquid hydrogen fuel allows the engine to be designed to operate relatively unaffected by the increasing Mach number across the entire flight operating range.

Although it is possible to use the hydrogen fuel directly in the thermodynamic cycle as the working fluid, it gives rise to material embrittlement problems in the hot, high-pressure condition. A helium loop is therefore introduced between the air and hydrogen loops as it is a good heat and work transfer medium which is passive to material attack and safe, i.e. non-toxic and non-flammable. The helium loop is the main power cycle, driving the turbines of the main turbo-compressor.

## 1.2 Technology development

The technology within Scimitar is based upon a mixture of current well-developed gas turbines practise and new leading edge heat exchanger technology. Both the temperature and pressure ranges within the engine are well within current practice, however substantial development is still required to bring long-life reliable hardware into practise.

As for the heat exchanger development, this was undertaken to complement and in some areas extend the work being pursued for Reaction Engines' spaceplane engine design (known as SABRE). The main engine precooler would make use of well-explored tubular technology whereas the preburner/HX3 heat exchanger would employ the use of ceramics, as the matrix design temperature is 1098K.

Scimitar also features a stator-less contra-rotating turbine, the efficiency of which is very important in precooled engines. The working fluid of hot helium is used to drive a relatively cold two-spool air compressor; this proves to be very well matched, the turbine behaving as though it were a conventional machine running at twice the speed.

The installation of the engine has to be designed carefully due to capture and pressure recovery characteristics of the intake. In particular the installation must include a bypass duct so that excess capture flow beyond that required by the core engine can be conducted to the bypass nozzle without passing through the core engine cycle. This bypass also includes a fan with a hub turbine which, when driven by the flow from the core engine, increases the mass flow and reduces the equivalence ratio leading to an effective subsonic high airflow engine. When reheated in the bypass duct, this provides the thrust-weight needed for take off. At higher Mach numbers (>2.5) the bypass fan windmills and the bypass duct acts like a ramjet with steadily reducing flow up to Mach 5 when all the flow then passes through the core engine. This is the direct opposite of a turbo-ramjet where the flow is steadily diverted from the core engine to the bypass ramjet system at the higher Mach numbers.

## 2. Basic precooled engine concept

At Mach 5 the air stagnation temperature of 'perfect air' is about 1320K and it is impractical to compress it directly to high pressures due to the work requirement and because the resulting compressor delivery temperature would be too high to handle. However, as outlined above, more subtle thermodynamic processes are possible when the fuel is liquid hydrogen. The possibilities this opens can be examined by considering the air and fuel entering the engine as a single thermodynamic system having enthalpy and entropy that are conserved during the air compression process.

Perfect gas relations are used to keep the derivations simple and to make the underlying principles clear. Upper case letters denote stagnation conditions and lower case static conditions. The enthalpy balance through the compression process is:

$$(\dot{m}C_p)_{air}(T_1 - T_s) = (\dot{m}C_p)_{H2}(T_f - T_i) \quad (1)$$

Where  $T_1$ ,  $T_s$  are the air entry and exit temperatures and  $T_i$ ,  $T_f$  are the hydrogen entry and exit temperatures.  $\dot{m}C_p$  is the thermal capacity of the appropriate flow. The entropy balance,  $\Delta S$ , through the compression is:

$$\Delta S = \dot{m}_{air} \left[ C_{Pair} \cdot \ln \left( \frac{T_s}{T_1} \right) - R_{air} \cdot \ln \left( \frac{P_s}{P_1} \right) \right] + \dot{m}_{H2} \left[ C_{PH2} \cdot \ln \left( \frac{T_f}{T_i} \right) - R_{H2} \cdot \ln \left( \frac{P_f}{P_i} \right) \right] \quad (2)$$

Where  $\dot{m}$  is the mass flow,  $C_p$  the specific heat,  $P$  the pressure and  $R$  the gas constant for the appropriate fluid. For a perfect cycle  $\Delta S = 0$ , otherwise  $\Delta S > 0$ . Substituting  $K_1 = (\dot{m}C_p)_{H2}/(\dot{m}C_p)_{air}$ ,  $\Delta s = \Delta S/\dot{m}_{air}$  and  $R = C_p(\gamma - 1/\gamma)$ , with  $\gamma_a$  and  $\gamma_h$  for air and hydrogen respectively, the above relations become:

$$T_1 - T_s = K_1(T_f - T_i) \quad (3)$$

$$\frac{\Delta s}{C_{Pair}} = \left( \ln \left( \frac{T_s}{T_1} \right) - \frac{(\gamma_a - 1)}{\gamma_a} \cdot \ln \left( \frac{P_s}{P_1} \right) \right) + K_1 \left( \ln \left( \frac{T_f}{T_i} \right) - \frac{(\gamma_h - 1)}{\gamma_h} \cdot \ln \left( \frac{P_f}{P_i} \right) \right) \quad (4)$$

Where  $\gamma = C_p/C_v$  is the ratio of heat capacities at constant pressure and constant volume.

For the moment assuming that  $\Delta s = 0$ ,  $T_1$  is given by the flight condition (Mach no = 5),  $T_i$  is given by the hydrogen storage and pumping conditions,  $P_i$  and  $P_f$  for the hydrogen are left as a design choice and that  $K_1$  is determined by the general requirements of efficient propulsion, see the box below. This leaves  $T_s$  and  $T_f$  as free variables to maximise the pressure ratio  $P_s/P_1$ . This optimum can be shown by standard methods of calculus to occur when  $T_s = T_f$ , both of which can then be determined from the enthalpy balance relation. The best attainable pressure ratio is then determined from the entropy equation. Without heat addition by combustion this is the very maximum pressure ratio that is thermodynamically allowed. At a more general level, the fact that the optimum occurs when  $T_s = T_f$  follows from thermodynamic considerations, since if this were not true, their temperature difference could be used to produce more work within the cycle.

**For example:**

Let  $\gamma_a = \gamma_h = 1.4$ ,  $T_1 = 1320K$ ,  $T_i = 35K$  (following pumping),  $\frac{P_f}{P_i} = 1$  (i.e. no pressure changes on the LH<sub>2</sub> side,  $K_1 = 0.4188$  (stoichiometric fuel-air ratio).

It then follows that  $T_5 = T_f = 940.7K$  and  $\frac{P_5}{P_1} = 38.04$ .

This is a very theoretical value and due to practical constraints the real values which can be achieved are very much smaller, by a factor 5 or so. We can also see that for the above example the compressor inlet temperature corresponding to the  $T_5$  delivery temperature would be about 333K for isentropic compression showing that the air will be pre-cooled by 987K before entering the compressor.

Hence by using this technique the compressor temperature regime becomes very conventional and the hydrogen fuel exit temperature is still relatively low while remaining at the full pump delivery pressure. At the same time, the equivalence ratio remains low (1.0 in the above idealised example) so that the engine can achieve close to the theoretical maximum specific fuel consumption. It remains to determine a practical cycle which can deliver the above thermodynamic result.

## 2.2 Theroretical limits to airbreathing specific impulse

The conservation of energy and momentum enable a quite accurate estimate to be made of the upper limits to the performance of all chemically fuelled air breathing engines. Consider the following ‘engine’:

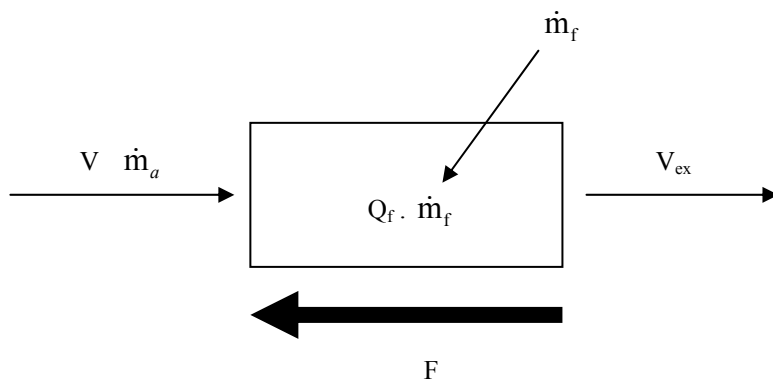


Figure 1: Simplified engine

The vehicle has a velocity relative to the air  $V$ . We take a frame of reference at rest relative to the engine. The flow of air entering the engine is  $\dot{m}_a$  and the fuel flow is  $\dot{m}_f$  which upon combustion releases  $Q_f$  joules/kg. The velocity of the exhaust is  $V_{ex}$ . The engine produces thrust  $F$  Newtons. The efficiency of conversion of the total non-thermal input energy to the engine to exhaust jet kinetic energy is  $\eta$ , therefore:

$$\text{Conservation of momentum: } F = (\dot{m}_a + \dot{m}_f) \cdot V_{ex} - \dot{m}_a \cdot V \quad (5)$$

$$\text{Conservation of energy: } (Q_f \cdot \dot{m}_f + \dot{m}_a \cdot \frac{V^2}{2}) \cdot \eta = (\dot{m}_a + \dot{m}_f) \cdot \frac{V_{ex}^2}{2} \quad (6)$$

After algebraic manipulation with air-fuel ratio =  $\dot{m}_a / \dot{m}_f$  leads to:

$$V_{ex} = \sqrt{\left( \frac{2 \cdot Q_f + V^2 \cdot afr}{1 + afr} \right) \cdot \eta} \quad (7)$$

$$F = \dot{m}_f \left( \sqrt{(1 + afr)(2 \cdot Q_f + V^2 \cdot afr)} \cdot \eta - V \cdot afr \right) \quad (8)$$

The effective exhaust velocity,  $\bar{V}_{eff} = F / \dot{m}_f$  is given by:

$$\bar{V}_{\text{eff}} = V \left( \sqrt{\left(1 + \text{afr}\right) \left( \frac{2 \cdot Q_f}{V^2} + \text{afr} \right)} \cdot \eta - \text{afr} \right) \quad (9)$$

It can be shown by differentiation, assuming constant  $\eta$ , there is an optimum value of air-fuel ratio that maximises  $\bar{V}_{\text{eff}}$  as long as the combustion is less than stoichiometric. Writing  $a = 2 \cdot Q_f / V^2$  the optimum air-fuel ratio is given by:

$$\text{afr} = \frac{1}{2} \left( \sqrt{\frac{(a-1)^2}{1-\eta}} - (a+1) \right) \quad (10)$$

Inserting this value into the  $V_{\text{eff}}$  equation then gives the optimum exhaust velocity. Using values for hydrogen,  $Q_f = 1.2 \times 10^8 \text{ J/kg}$ , stoichiometric air-fuel ratio = 34.29 and a typical efficiency of  $\eta = 0.8$  we can examine the variation of parameters with Mach number. In Figure 2 below it can be seen that the optimum Equivalence Ratio rises monotonically with Mach number, reaching 1.0 above approximately Mach 7. It can be shown by direct substitution of values that  $V_{\text{eff}}$  is not too seriously degraded by operating at  $\text{ER} = 1$  down even to Mach 4 (Figure 3), while it has the beneficial effect of increasing the thrust per unit air flow, producing a more compact engine at the expense of fuel consumption. This analysis enables a suitable  $K_1$  value to be selected for the pre-cooled engine which will be a compromise to realise a practical cycle while not unduly reducing the fundamental engine performance. This is addressed below.

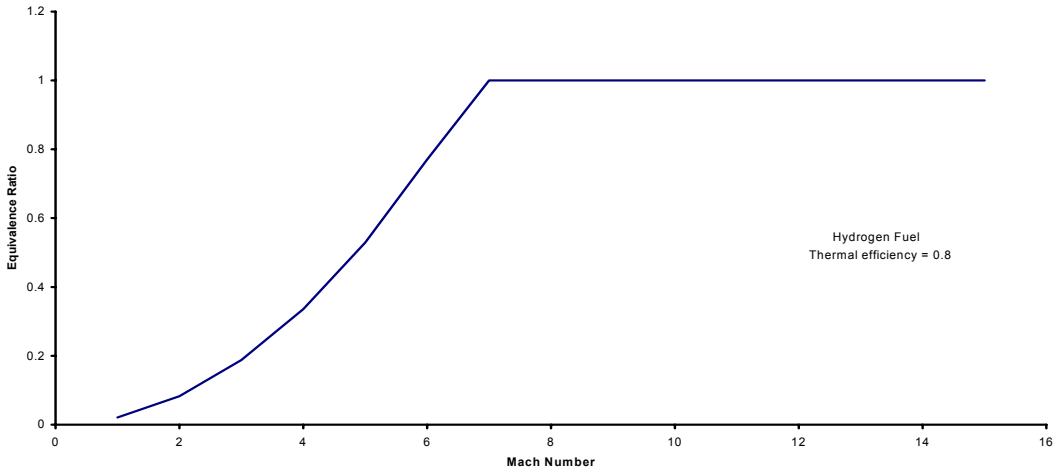


Figure 2: Optimum Equivalence Ratio vs. Mach Number

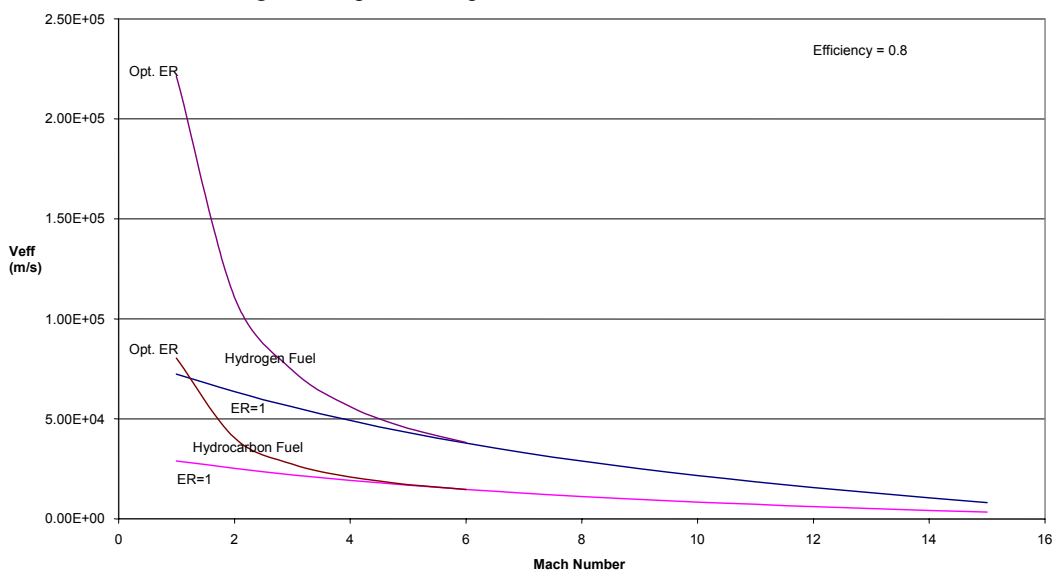


Figure 3: Optimum Effective Exhaust Velocity vs. Mach Number

### 3. Cycle synthesis

The theory above shows that a cycle is possible but gives no guidance as to its configuration, of which there are several. Fortunately, only a few are practical and all involve considerable heat exchange in which, in order to minimise entropy rise, the heat exchangers must have matched capacity ratios. It can be shown that this requires the ideal overall air-fuel capacity ratio to be a rational number. At the same time the air-fuel ratio should not be far from the optimum derived in the section above. For the Scimitar engine a capacity ratio  $K_1 = 1/3$  was fixed after some iteration. This corresponds to an air-fuel ratio of 43.087 or Equivalence Ratio = 0.7959. The optimum ER would be expected to be about 0.55 based on the ideal propulsion analysis above. Hence, Table 1 below shows that the selected capacity ratio gives a higher fuel consumption relative to the ideal performance by about 2%

Table 1: The theoretical variation of  $V_{\text{eff}}$  as a function of ER at  $V=1500\text{m/s}$  and  $\eta = 0.8$

Equivalence Ratio	0.55	0.7959	1.0
$V_{\text{eff}}(\text{m/s})$	45302	44383	43190

If a simple counter flow pre-cooler were used, the helium exit temperature would approach the stagnation air temperature and the heat transfer surface would, of necessity, approach this temperature also bringing significant materials problems. The capacity ratio of the high temperature portion of the pre-cooler (HX1) is therefore reduced to 1:3 air to helium so as to keep the helium temperature to about 1000K. In the colder part of the pre-cooler (HX2) the capacity ratio is unity.

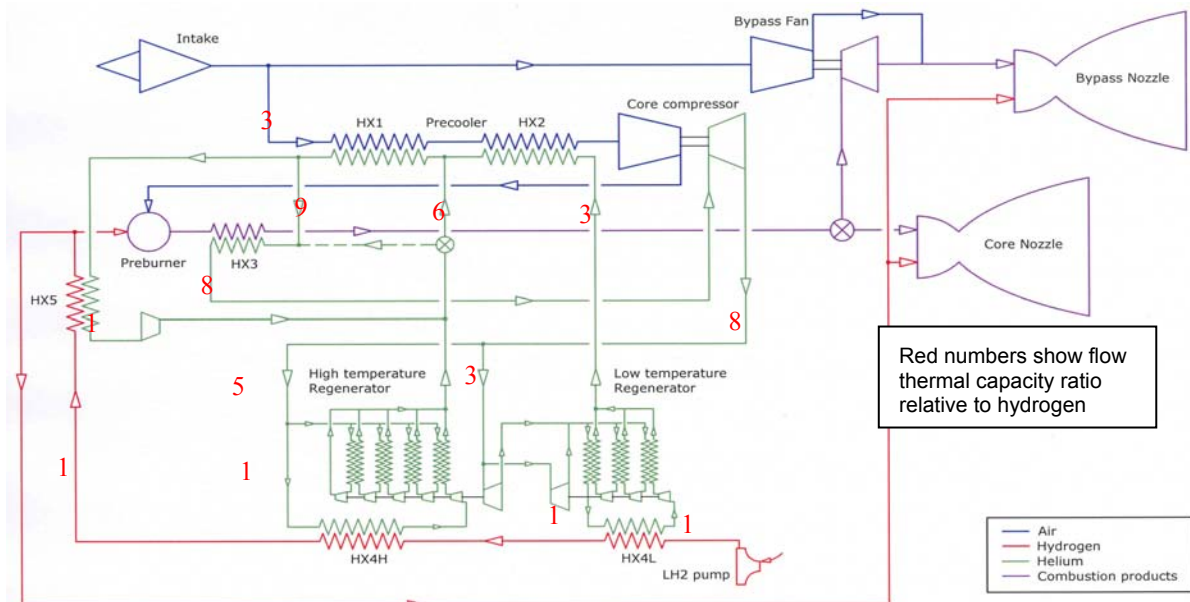


Figure 4: Scimitar basic cycle

Since the capacity ratio of the hydrogen to air is 1:3, it follows that part of the heat rejection helium-to-hydrogen is at a capacity ratio 3:1 for the flow loop through HX2 and the helium-to-hydrogen is at a capacity ratio of 9:1 through that part of the helium flow which passes through HX1. This involves splitting the helium flow into the appropriate number of parallel paths and cooling them in tandem in the regenerators. The cycle is shown in Figure 4.

The regenerator configuration appears complicated but is in fact simple, the apparent complexity coming from the number of parallel flow paths. Each of the separate flows is in matched capacity rate with the hydrogen, but also with the other helium streams. The capacity flow rate relative to hydrogen is shown on Figure 4 in red numerals. Following compression of each of the cold helium streams they are still at low temperatures and can be used to cascade the cooling, helium-to-helium, between each individual stream. It is then only necessary to cool the helium with the hydrogen for that helium stream which leaves at the lowest temperature, the overall enthalpy balance being maintained whilst simplifying the heat exchanger configuration.

The cycle needs to incorporate a pre-burner releasing some of the chemical potential of the fuel to compensate the loss of enthalpy in the airflow at lower Mach numbers. This maintains the helium at constant temperature to drive the turbo-compressor independent of Mach number so that the cycle is, in effect, always at the Mach 5 condition.

An air bypass is necessary in a hypersonic aspirated engine installation to match the intake capture flow to the demanded core engine flow over the off-design Mach number range. Without this there will be large drag penalties due to air spillage in this flight regime. The bypassed air is passed through a combustion system in the duct in order to heat the air and gain thrust from it during supersonic acceleration. It is in effect a bypass ramjet, the thrust from which falls to zero at the engine design operating condition.

Although the Scimitar engine is configured to cruise efficiently at Mach 5 it also has to operate effectively at subsonic Mach numbers in order to over-fly populated areas without nuisance ('sonic boom') and also be capable of takeoff and landing within the international environmental standards on noise and emissions. In order to meet the subsonic requirements above, a fan has also been incorporated into the bypass duct of the Scimitar installation. This is driven by a hub turbine using the core engine airflow which is diverted away from the core nozzle. The combined airflow downstream of the fan can then be heated in the bypass combustion system in reheat to produce thrust via the bypass nozzle, the core nozzle being empty. The engine is optimised to give the best specific thrust at mach 0.9 without any heat addition in the bypass burner, although this is still well below the theoretical optimum predicted by the theory in section 2 above at Mach 0.9.

### 3.2 Scimitar Engine Configuration

The preliminary Scimitar configuration is shown in Figure 5. It employs a three shock intake to give an intake  $\eta_{KE} = 0.9$  which is expected to be readily achievable. The precooler consists of six segments, each made from approximately 70 modules; and limits the compressor inlet temperature to 635K. The compressor is a counter-rotating two spool machine with an overall pressure ratio of 4.07. It is driven by a stator-less counter rotating helium turbine. The regenerator heat exchangers and circulators are arranged around the compressor as shown in Figure 6. The exhaust from HX3 can be directed by means of a diverter valve either to the core combustion chamber and nozzle (supersonic or P mode) or to through the hub turbine of the fan to the bypass burner (subsonic or B mode). The bypass nozzle has a petal arrangement enabling its area to be varied over a wide range with maximum opening for takeoff at maximum bypass burner equivalence ratio to fully closed for Mach 5 supersonic cruise. In B mode the two stage fan has a pressure ratio of 1.8. In P mode the fan windmills to give minimum pressure loss in the bypass flow.

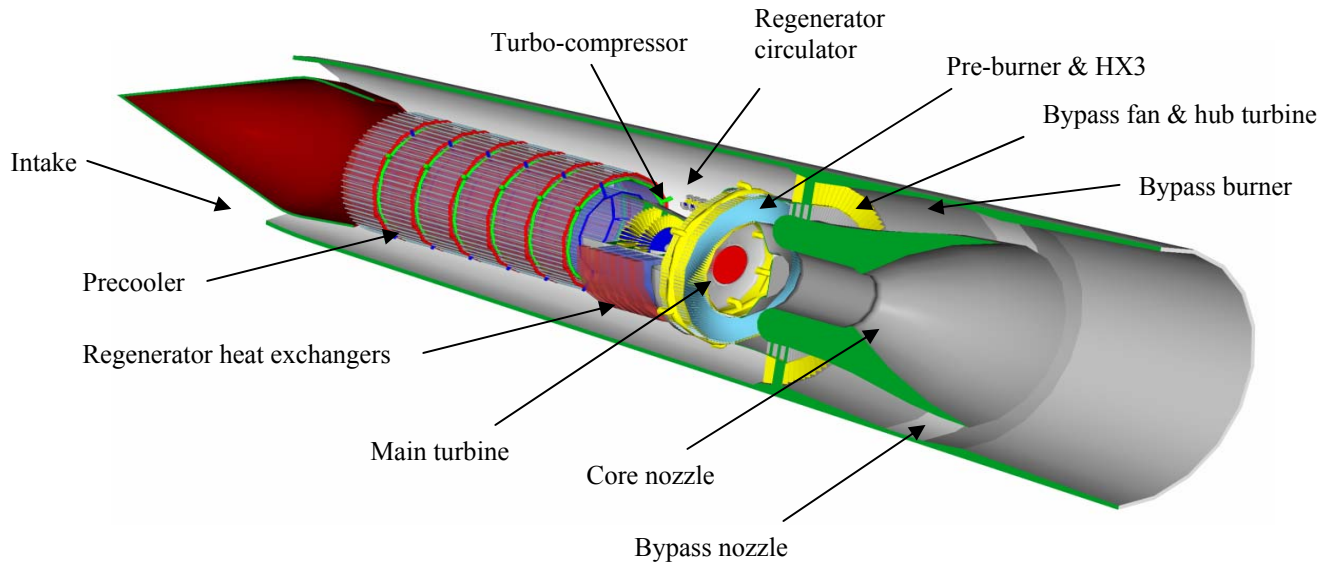


Figure 5: Section through Scimitar Installation

### 4. Cycle parameters and engine performance

The design system pressures and temperatures at Mach 5 are shown on the cycle diagram, Figure 6. These were derived taking into account the practical efficiencies of the cycle components. The turbine power loop is designed to

operate at constant pressure and temperature ratio's at all operating points, the power level being varied by changing the helium content of the loop and hence the system pressure. This in turn changes the power loop mass flow in direct proportion to the pressure and the turbine power is, to a first order, directly proportional to the helium mass flow since the temperature drop in the turbine is constant.

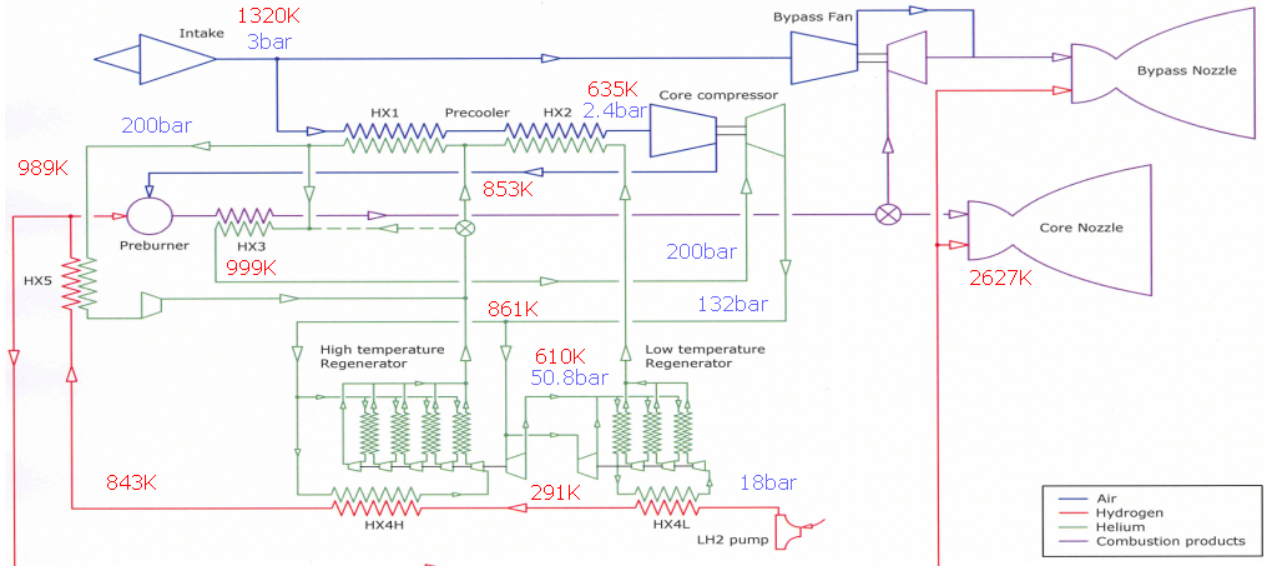


Figure 6: Nominal cycle parameters at Mach 5

A simple engine computer model was created using the above cycle as the basis and assuming that the compressor operated at constant non-dimensional mass flow,  $Q = \dot{m}\sqrt{T_4}/P_4$ . This enabled the scale of the engine to be fixed, and from the intake characteristics determine the compressor airflow at any flight condition. Combining this with a vehicle trajectory model, the engine operating parameters could be derived for a typical antipodal mission. It should be noted that this model was based on a number of assumptions, one being the nozzle design and performance. As described above, Scimitar has two nozzles, one for the bypass and the other for the core engine. For efficient operation it is essential that these nozzles have the correct throat area to pass the flow under the upstream pressure and temperature conditions, and the correct exit area to expand them efficiently to prevailing ambient conditions. Through performing initial calculations on the ideal nozzle throat and exit areas required on the climb-out and landing flight path profiles, it was established that the required bypass and core engine exit areas move opposite to each other and that a constant area base could be roughly partitioned to provide the exit area required by each nozzle. This led to the concept of a nozzle with petals which when closed complete the core engine contour, but when open create the bypass nozzle throat area and an annular bypass nozzle.

Table 2: Scimitar engine performance

Altitude (m)	Mach No	Equiv. Ratio	Thrust (N)	Airflow kg/s	Air-fuel ratio	Flight Phase
5.3	0.329	0.8	372,254	519.9	42.87	Runway acceleration with reheat
1230	0.408	0.407	248,134	477.0	84.28	Subsonic acceleration with reheat
16577	2.5 (B-mode)	0.7	272,771	284.2 (intake spilling)	48.98	engine mode change; subsonic phase
16577	2.5 (P-mode)	0.7	313,105	349.5 (full capture)	48.98	engine mode change; supersonic phase
<b>5900</b>	<b>0.9</b>	<b>0.0749</b>	<b>81,873</b>	<b>390.4</b>	<b>458.0</b>	<b>subsonic cruise</b>
<b>25400</b>	<b>5.0</b>	<b>0.8</b>	<b>168,348</b>	<b>173.6</b>	<b>42.87</b>	<b>supersonic cruise</b>

This concept required further investigation and analysis in order to reach a proper design and have confidence in its accurate performance parameters. In subsonic mode the internal pressure of the jet core may be depressed below ambient, resulting in substantial induced base drag. In supersonic mode the design needs to minimise the shock losses as the two separate flows accommodate within the same nozzle. The dual flow mode is only present during

vehicle acceleration and a practical nozzle which performed slightly less than the ideal would be acceptable. In cruise modes only one nozzle or the other, i.e. bypass or core engine, is in operation. The mechanical design is complex and will require a substantial study to derive the pressure and thermal loads, structure, cooling and actuation details.

The performance analysis also revealed that when flying the vehicle between Mach 1.2 and 2.5 with the engines operating in B mode, it is necessary to fore-spill air from the intakes with the current nacelle design. This is due to the engine demand being slightly miss-matched to the intake capture at this flight condition. An approximate correction was made to the vehicle drag to accommodate this effect. A revised nacelle design would be able to mostly eliminate this problem. Some performance figures for a single Scimitar engine are shown in Table 2 for specific points on the reference trajectory. In this table it is assumed that the engines change mode at Mach 2.5. Parameters at the two **design** cruise conditions are also shown in bold.

## 5. Contra-rotating Helium turbine

A contra-rotating turbine has successive blade rows that spin in opposite directions, transmitting their power to two counter rotating output shafts, one to each compressor spool. This design evidences mechanical challenges that prevent their extensive use: bearings rotating at high peripheral speeds, unconventional assemblies, high seal leakage flows. Figure 7 displays the blade to blade view of the turbine together with the velocity triangles. The first stage is a conventional turbine stage comprising a vane plus a blade row. The outlet flow of rotor 1 ( $V_{3,R1}$ ) has a rather high swirl and relative flow velocity ( $W_{3,R1}$ ), thanks to the contra-rotation in the next blade row the relative inlet velocity (and swirl) is rather small ( $W_{2,R2}$ ). In turbines with co-rotating rotors, a stator vane is required to deflect the flow in the sense of rotation to reduce the rotor inlet velocity in the subsequent blade rows. Clearly the use of contra-rotating turbines results in considerable mass and size savings. In comparison with a conventional high reaction turbine similar stage loading factors can be achieved with lower rotor turning, resulting in higher efficiencies. Additionally this design choice eliminates gyroscopic effects, and reduces cooling requirements.

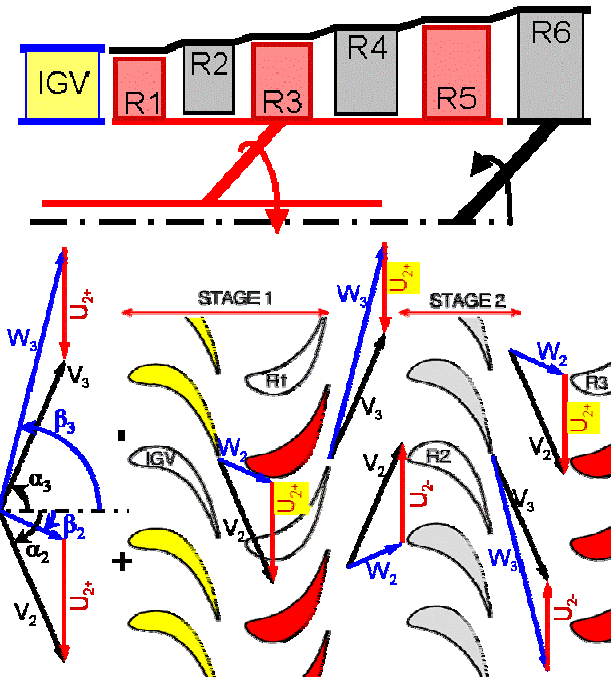


Figure 7: Velocity triangles in a contra-rotating turbine.

Furthermore the use of the contra-rotation enables a better matching of the helium turbine to the air compressor compensating their disparity in molecular weight. The  $C_p$  of helium is 4.5 times that of air, thus the temperature drop in a helium turbine is 4.5 times lower for an identical enthalpy drop. The heat capacity ratio ( $\gamma$ ) of helium is 20% higher than that of air; hence the pressure ratio in a helium turbine is about 20 times lower for the same work. The pressure and temperature change is very small along the machine axis, so the blade height remains nearly unaltered. In conventional gas turbines where the same working fluid is employed in the compressor and turbine the speed of sound are within a factor of 2 (being related by  $\sqrt{T}$ ) with the result that the turbine design is able to exploit high flow Mach numbers before being limited by the centrifugal stresses. For Scimitar the speed of sound in the helium

turbine is 3.6 times higher than the air compressor. Since the relatively low speed of sound in the compressor determines the spool speed a conventional turbine design would result in a low work per stage. However, by contra-rotation high outlet swirl angles are allowed resulting in high work extraction.

The requested shaft power in each axis is around 32 MW, the axis counter rotate at around 11000 RPM. The helium mass-flow available is about 90 kg/s, with a mean diameter of around 250 mm. The turbine inlet total pressure and temperature are 200 bar and 1000K. Three turbines were designed and optimized from a preliminary 1D design with an IGV and six contra-rotating rotors, with a polytropic total to total efficiency of 90.9 %. Detailed studies allowed a significant reduction in the number of blade rows. The numerical analysis comprised: a mean line design for the definition of the aerodynamic and thermodynamic properties of the flow, a two dimensional design of the blades, a three dimensional optimization and a stress calculation. The chosen solution is a balance between maximum efficiency / acceleration across the blade row / periodicity and minimum turbine exit swirl. The constraints to respect were: the airfoil turning should not exceed 130 deg., the size of the machine should be kept small and the periodicity across the stages should be guaranteed in order to simplify the blades design. The following parameters were evaluated: number of stages, blade height, degree of reaction, work distribution across the stages, rotational speed. A decrease in the number of stages results in lower efficiency (see Table 3, high turnings and high turbine outlet swirl). Furthermore, to re-establish the periodicity in the velocity triangles it is necessary to decrease the degree of reaction. Once the number of stages is fixed, the higher the degree of reaction the higher the efficiency. For the 3 turbines all the blade rows have been designed in 2D and 3D (radially stacked). The initial profile was obtained using an inverse code. This first design is then re-scaled to the correct chord and fitted with Bezier curves. An optimization procedure (based on genetic algorithms and artificial neural networks) was launched to provide 2 airfoils at hub, mid-span and tip.

Table 3 Efficiency, stage loading and flow factor of the three turbines.

	$\alpha_{2 \text{ RI}}$ [deg.]	$\alpha_{3 \text{ Rlast}}$ [deg.]	$\Delta H/U^2$	$V_{ax2}/U$	$\eta_{\text{POLY TT}}$
6-rotor	43.5	-36	1.6	0.8-1.0	90.0
4-rotor	36.3	-34.8	2.0-2.1	0.7-0.8	93.7
3-rotor	2.3	10.1	1.7-4.7	0.7-1.0	91.3
2-rotor	68.8	63.4	4.4-4.5	0.8-0.9	86.8

A configuration with only two rotors, each delivering 32 MW, is the most compact machine with very high stage loading factor ( $\Psi \approx 4.4$ ). Figure 8 sketches the three configurations with two to four rotors. The proposed three rotor turbine does not have an IGV nor a de-swirler delivering an efficiency of 91.3 %. This very compact design may however encounter problems during the start up.

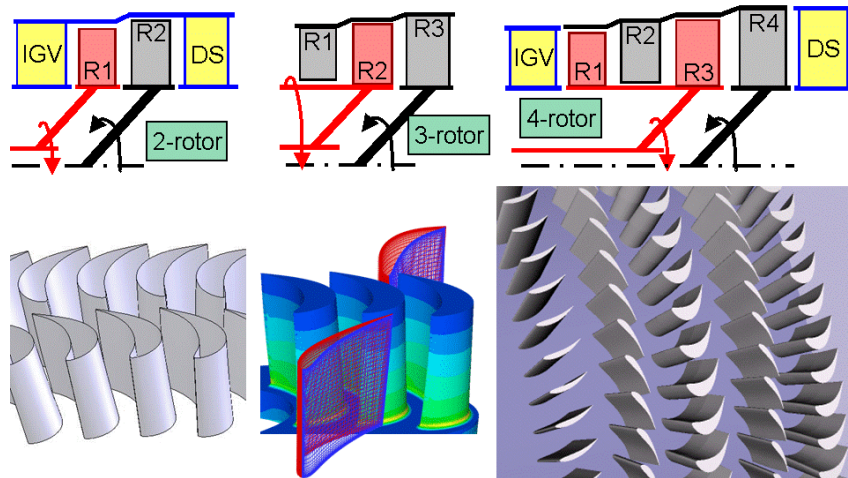


Figure 8: The three different contra-rotating turbines considered.

The selected geometry has 4 rotors. The IGV turns the flow only 31deg., in conventional turbines this value ranges between 65 to 73 deg. To limit the development cost of the turbine the next alternative investigated is to have only periodic conditions in each axis. Namely rotors 1 and 3 have the same velocity triangles, while in the second shaft rotor 2 and 4 are similar. The turbine has acceptable acceleration rates ( $M_3/M_2$ ) ranging between 1.6 and 3.2. If the rotational speed would be decreased 10% the relative inlet flow angle to the first rotor 1 would be reduced by 5 deg. Thus, blades able to perform without separation at  $\pm 10$  deg. incidence are suitable to ensure a good off-design

operation. 3D 5-row calculations were performed to evaluate the design and off-design operation. Figure 10 presents the total-to-static isentropic efficiency. Increasing the rotational speed raises the efficiency, while they become less insensitive to variations in the mass-flow. At nominal RPM the efficiency continuously decreases with the mass-flow from 91.2 to 89.9%. By changing the pressure ratio or the RPM the incidence to the rotors are changed, while the rotor outlet relative angle is little affected. Figure 10-right shows the turning of rotor 2 and rotor 3 for the different conditions, the turning in rotor 2 and 4 is nearly identical, the variations in rotor 1 are much lower than in rotor 3. When the mass-flow increases (the pressure ratio is lowered) the incidence increases (towards negative values) in rotor 1 and 3, resulting in an increased turning. Similarly in rotors 2 and 4 the turning increases reducing the pressure ratio, in consequence, at the lowest pressure ratios the flow separates in the blade crown. Reducing the RPM the turning is increased, which explains the reduction in efficiency. In parallel with the aerodynamic optimization, the mechanical integrity of the airfoils was assessed. The blade stresses and displacements were computed using a finite element model (FEM) solver (SAMCEF).

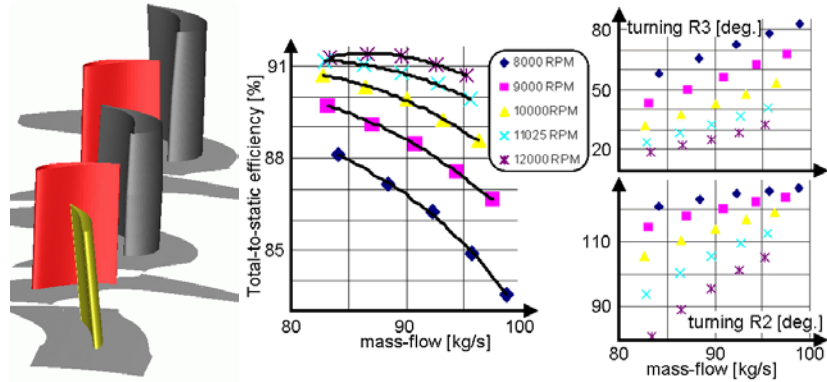


Figure 10: 3D N-S simulation of the turbine at off-design conditions.

## 6. Conclusions

A preliminary design investigation of a precooled engine employing hydrogen fuel suggests that it would deliver close to ideal performance at Mach 5 and be capable of yielding antipodal range in combination with a suitable airframe. The same engine would be capable of good fuel consumption in subsonic cruise as well as a quiet take-off meeting current international standards. This would remove the two major obstacles which prevented Concorde entering World-wide service, namely limited range and high take-off noise.

The engine poses several design and development challenges in intakes, heat exchangers and nozzles, although none of these require fundamental breakthroughs in technology for their realisation. The main difference between the Scimitar engine and the well investigated SABRE spaceplane engine is the design lifetime, 15,000 hours compared to 50 hours. Apart from this, the Scimitar requirement is alleviated by reduced mass sensitivity relative to SABRE. The major problem which was found in the course of this study is the formation of NO<sub>x</sub> at the high combustion temperature required in Mach 5 cruise. This will be the focus of future R&D for this engine. Apart from the issue of NO<sub>x</sub> formation the engine is considered a practical development from known technology.

## 6. Acknowledgments

This work was performed within the ‘Long-Term Advanced Propulsion Concepts and Technologies’ (LAPCAT) project investigating high-speed air-breathing propulsion. LAPCAT, coordinated by ESA-ESTEC, is supported by the EU within the 6th Framework Programme Priority 1.4, Aeronautic and Space, Contract no.: AST4-CT-2005-012282. Further info on LAPCAT can be found on:  
<http://www.estec.esa.int/techresources/lapcat>.